

# Nonlinear MPC for full-pose manipulation of a cable-suspended load using multiple UAVs

Sihao Sun, Antonio Franchi

**Abstract**—Using multiple UAVs to manipulate the full pose of an object is a promising capability in many industrial applications, such as autonomous building construction and heavy-load transportation. Among various methods, manipulation via cables excels in mechanical simplicity and ease of use, but is challenging from a control perspective. Existing centralized control methods either neglect the dynamic coupling between UAVs and the load or resort to a cascade structure, which limits the operational speed and cannot guarantee safety. In this work, we propose a centralized control method that uses nonlinear model predictive control. This control method takes into account the full nonlinear model of the load-UAV system, as well as the constraints of UAV thrust, collision avoidance, and ensuring all cables are taut. By taking into account the above factors, the proposed control algorithm can fully exploit the performance of UAVs and facilitate the speed of operation. We demonstrate our algorithm through 6-DoF simulations to achieve fast and safe manipulation of the pose of a rigid-body payload using multiple UAVs. **NB: This is a draft version. Full paper will be released soon.**

## I. INTRODUCTION

### A. Background and motivation

- Collaborative manipulation is a promising capability in many industrial applications, given the fact that the payload capacity of a single UAV is limited.

### B. Related works

- Works for single UAV and a point-mass sling load (e.g., [1], [2]).
- Works for multi-UAVs with a point-mass sling load (e.g., [3], [4], [5]).
- Works for multi-UAVs with a rigid-body sling load (e.g., [6], [7], [8], [9]).
- Existing works for multi-UAVs manipulating the full pose of a rigid-body load with suspended cables cannot simultaneously consider the full-nonlinear dynamic model of the load-UAVs system, and the thrust limitation of each UAV, as well as other constraints such as taut cable, and collision avoidance.

### C. Contribution of this work

- A centralized control algorithm that can automatically exploit the redundancy of the load-UAVs system.
- Fully explore the load-UAVs system's nonlinear dynamics, and consider system constraints.
- Formulate the system model to allow real-time optimization.

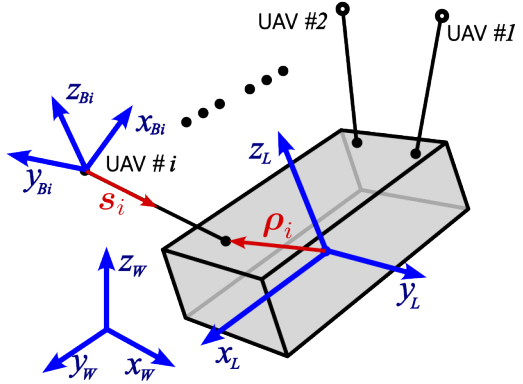


Fig. 1. Coordinate systems definition.

## II. PRELIMINARY

### A. Problem Formulation

The system comprises  $n$  UAVs and a single rigid-body load. There is a coordinate system  $\mathcal{L} = \{O_L, x_L, y_L, z_L\}$  attached to the load with the origin located at the centre of mass. For each UAV, there is a body-fixed frame  $\mathcal{B}_i = \{O_{B_i}, x_{B_i}, y_{B_i}, z_{B_i}\}$  attached where  $O_{B_i}$  is at the center of mass of the  $i$ th UAV and  $z_{B_i}$  points at the thrust direction. The position of the load with respect to the inertial frame  $\mathcal{I}$  is denoted by  $\mathbf{p}$ , and the orientation is denoted by  $\mathbf{R} \in \text{SO}(3)$ . Similarly, the position and orientation of the  $i$ th UAV is denoted by  $\mathbf{p}_i$  and  $\mathbf{R}_i \in \text{SO}(3)$  respectively. The angular rate and

Each UAV is connected to the load through a cable with a length of  $l_i$ , where subscription  $i \in \mathbb{N}_+ \leq n$  is the UAV index. Both sides of the cable are hinge connections, with one side connected to the centre of mass of the UAV and another side connected to an arbitrary point of the load, displacing from its centre of mass by  $\rho_i$ . The cable tension is denoted by  $t_i \leq 0$ .

The UAV considered in this work are *uni-directional Thrust* platforms, whose collective thrust can only vary along one direction (i.e.,  $z_{B_i}$ ). Examples are helicopters and multi-rotor drones whose rotors are coplanar. These platforms can generate moments to change their thrust direction, and consequently, change their position in the inertial frame. The objective of the controller designed in this paper is to generate the collective thrust  $f_i$  and moment  $\tau_i$  of all the UAVs, such that the position and attitude (full pose) of the load can follow a given value.

## B. Modeling

1) *Load-cable model*: We model the load using a 6 DoF rigid-body dynamic model:

$$\dot{\mathbf{p}} = \mathbf{v} \quad (1)$$

$$\dot{\mathbf{v}} = - \sum_{i=1}^n t_i \mathbf{s}_i / m + \mathbf{g} \quad (2)$$

$$\dot{\mathbf{R}} = \mathbf{R} \boldsymbol{\omega}_x^L \quad (3)$$

$$\dot{\boldsymbol{\omega}}^L = \mathbf{I}_L^{-1} \left( -\boldsymbol{\omega}^L \times \mathbf{I}_L \boldsymbol{\omega}^L + \sum_{i=1}^n \left( \mathbf{R}^T \mathbf{s}_i \times \boldsymbol{\rho}_i^L \right) \right) \quad (4)$$

The mass-less cable is modelled with only kinematics considered, up to angular accelerations. For the  $i$ -th cable, we have

$$\dot{\mathbf{s}}_i = \mathbf{r}_i \times \mathbf{s}_i \quad (5)$$

$$\ddot{\mathbf{r}}_i = \mathbf{c}_i \quad (6)$$

2) *UAV model*: The UAV considered in this paper are uni-directional UAVs, meaning that only thrusts along a single direction (defined as  $z_i$  of the vehicle) are generated, examples are helicopters and quadrotors. In this work, we use a rigid-body model to represent the kinematics and dynamics of the UAV. Specifically, the model of the  $i$ -th UAV is:

$$\dot{\mathbf{p}}_i = \mathbf{v}_i \quad (7)$$

$$\dot{\mathbf{v}}_i = (f_i \mathbf{z}_i + t_i \mathbf{s}_i) / m_i + \mathbf{g} \quad (8)$$

$$\dot{\mathbf{R}}_i = \mathbf{R}_i \boldsymbol{\omega}_{i,\times}^{B_i} \quad (9)$$

$$\dot{\boldsymbol{\omega}}_i^{B_i} = \mathbf{I}_i^{-1} \left( -\boldsymbol{\omega}_i^{B_i} \times \mathbf{I}_i \boldsymbol{\omega}_i^{B_i} + \boldsymbol{\tau}_i \right) \quad (10)$$

## C. Kinematic Constraints

Since each UAV is constrained at the end of the corresponding cable, for the  $i$ -th UAV, we have the following kinematic constraint:

$$\mathbf{p}_i = \mathbf{p} + \mathbf{R} \boldsymbol{\rho}_i^L - l_i \mathbf{s}_i \quad (11)$$

These constraints render the UAV states dependent on the load-cable model. This is also known as the differential flatness of the (multi-)UAV-load-cable system [10]. The UAV states can be derived as algebraic functions of the load pose and cables' orientations. For the optimization problem in the next section, we need to set constraints on the collective thrust of each UAV to fulfil its physical limitation. Therefore we derive the thrust of each UAV using the kinematic constraints.

By taking the second-order derivative of both sides of (11) and substituting (3)-(6) to it, we have

$$\begin{aligned} \dot{\mathbf{v}}_i &= \dot{\mathbf{v}} + \mathbf{R} (\dot{\boldsymbol{\omega}}_i^{B_i} \times \boldsymbol{\rho}_i^L + \boldsymbol{\omega}^L \times (\boldsymbol{\omega}^L \times \boldsymbol{\rho}_i^L)) \\ &\quad - l_i \dot{\mathbf{r}}_i \times \mathbf{s}_i - l_i \mathbf{r} \times (\mathbf{r} \times \mathbf{s}_i) \\ &= (f_i \mathbf{z}_i + t_i \mathbf{s}_i) / m_i + \mathbf{g} \end{aligned} \quad (12)$$

Through simple algebra, we have

$$\begin{aligned} f_i \mathbf{z}_i &= \mathbf{f}_i = m_i [\dot{\mathbf{v}} + \mathbf{R} (\boldsymbol{\omega}^L \times \boldsymbol{\rho}_i^L + \boldsymbol{\omega}^L \times (\boldsymbol{\omega}^L \times \boldsymbol{\rho}_i^L)) \\ &\quad - l_i \dot{\mathbf{r}}_i \times \mathbf{s}_i - l_i \mathbf{r} \times (\mathbf{r} \times \mathbf{s}_i)] \\ &\quad - t_i \mathbf{s}_i - \mathbf{g} \end{aligned} \quad (13)$$

$$f_i = \|\mathbf{f}_i\| \quad (14)$$

$$z_i = \mathbf{f}_i / f_i \quad (15)$$

Collisions between UAVs and cables need to be avoided for safety reasons, here we express the distance between  $i$ -th UAV and the  $j$ -th cable as

$$\begin{aligned} d_{ij} &= (\mathbf{p}_i - \mathbf{p}_j) \times \mathbf{s}_i \\ &= \mathbf{R} (\boldsymbol{\rho}_i^L - \boldsymbol{\rho}_j) + (l_j \mathbf{s}_j - l_i \mathbf{s}_i) \times \mathbf{s}_i \end{aligned} \quad (16)$$

## III. METHODOLOGY

The control algorithm designed in this section aims at controlling the full pose of the load to a reference, by generating thrust and torque commands for all the UAVs. In the meantime, we guarantee safety by incorporating the thrust constraints and the collision constraints. This will help to fully exploit the capability of each UAV. The control diagram is illustrated in Fig. 1.

### A. Nonlinear model predictive control

The nonlinear model predictive controller utilizes the load-cable model. The states and inputs of this model are defined as:

$$\mathbf{x} = [\mathbf{p}, \mathbf{v}, \mathbf{R}, \boldsymbol{\omega}^B, \mathbf{s}_1, \mathbf{r}_1, \dot{\mathbf{r}}_1, \dots, \mathbf{s}_n, \mathbf{r}_n, \dot{\mathbf{r}}_n] \quad (17)$$

$$\mathbf{u} = [\mathbf{c}_1, t_1, \dots, \mathbf{c}_n, t_n] \quad (18)$$

Then the following optimal control problem (OCP) is solved in each control step of nonlinear MPC:

$$\min \quad J = \int_{\tau=0}^{\tau_f} \frac{1}{2} \|\mathbf{y}_{ref} - \mathbf{y}\|_W^2 + \|\boldsymbol{\sigma}\|_W^2$$

s.t. *Initial condition*:

$$\mathbf{x}_0 = \mathbf{x}$$

*Dynamics*:

$$(1) - (4)$$

$$(5)(6) \text{ for } i = 1 \dots n$$

*Taut cable constraint*:

$$0 \leq t_{min} \leq t_i \leq t_{max}$$

*Thrust constraint*:

$$f_{min} \leq f_i \leq f_{max} \text{ for } i = 1 \dots n$$

*Collision avoidance constraint*:

$$d_{min} \leq d_{ij} \text{ for } i = 1 \dots n$$

where  $\mathbf{y}_{ref}$  are the pose reference of the load, namely

$$\mathbf{y}_{ref} = [\mathbf{p}_{ref}, \mathbf{q}_{ref}] \quad (19)$$

Note that the above OCP includes a taut cable constraint to prevent cable slack in the predicted trajectory. The thrust constraint and the collision avoidance constraint are also included, where  $f_i$  and  $d_{ij}$  have been derived respectively in (14) and (16).

By solving the above OCP we can obtain the optimal states and control along the discrete nodes. We use  $\bar{x}$  and

$\bar{u}$  to express the corresponding array of optimal states and inputs, and  $\mathbf{x}|_k$  ( $k \in [0, N]$ ) to indicates the variables in the prediction horizon at node  $k$ . Given  $\bar{x}$  and  $\bar{u}$ , we can obtain the thrust and its direction of all the UAVs along the trajectory using (13)-(15). At the  $k$ -th node, they are denoted respectively by  $f_i|_k$  and  $\mathbf{z}_i|_k$ .

The inputs of the NMPC are not fed into the controller. Instead, we use  $f_i|_k$  and  $\mathbf{z}_i|_k$  generated by the NMPC as the reference of the UAV controllers. According to (13),  $f_i|_k$  and  $\mathbf{z}_i|_k$  have algebraic relationship with states of the NMPC. Therefore, their values on the first node on the predicted trajectory are equal to the current thrust and its direction. In practice, we use their values on the most recent node on the predicted trajectory for simplicity. Then for the  $i$ -th UAV, we have

$$f_{i,ref} = f_i|_1 \quad (20)$$

$$\mathbf{z}_{i,ref} = \mathbf{z}_i|_1 \quad (21)$$

Then the angular rate of the  $i$ -th UAV along the trajectory can be calculated through finite differentiation, yielding

$$\boldsymbol{\omega}_i|_k = (\mathbf{z}_i|_k + \mathbf{z}_i|_{k+1}) \times (\mathbf{z}_i|_{k+1} - \mathbf{z}_i|_k) / 2\Delta T \quad (22)$$

Note that it is also possible to obtain  $\boldsymbol{\omega}_i|_k$  through algebraic derivations by taking the derivative of both sides of (13), but this operation requires the knowledge of  $\dot{t}_i$  as well as  $\dot{f}_i$  which still need to be acquired through finite differentiation along the predicted trajectories. Hence we chose to calculate  $\boldsymbol{\omega}_i|_k$  directly via (22).

Specifically, for the  $i$ -th UAV, we have

$$\boldsymbol{\omega}_{i,ref} = \boldsymbol{\omega}_i|_0 \quad (23)$$

which will be used by the inner-loop attitude controller of each UAV.

Note that the yawing motion of each UAV is not included in the optimal trajectory (Here we define yaw as the angle that each UAV rotates about its thrust direction from a pre-defined reference direction, such as toward the east). This is because the yaw angle does not affect the thrust generated by each UAV and consequently brings no effect to the forces on the load.

In practice, the reference heading can be set for other purposes such as better perception accuracy [11]. Denote the yaw angle of the  $i$ -th UAV as  $\theta_{i,ref}$ , then from the definition of quaternion, we have the reference attitude of the  $i$ -th UAV in the quaternion form

$$\mathbf{q}_{i,ref} = \begin{bmatrix} \cos(\theta_{i,ref})/2 \\ \mathbf{z}_{i,ref,x} \sin \theta/2 \\ \mathbf{z}_{i,ref,y} \sin \theta/2 \\ \mathbf{z}_{i,ref,z} \sin \theta/2 \end{bmatrix} \quad (24)$$

### B. Inner-loop controller of each UAV

The inner-loop controller computes the thrust that needs to be generated from the rotors of each UAV, given reference thrust, attitude, and body rates. The choice of this inner-loop controller is not unique, examples are geometric attitude controller [12], or quaternion-based controller [13]. In this work,

we choose a quaternion-based controller that separates the thrust direction tilt and the yaw [14]. Here we briefly write down the key equations of this controller for readability. We refer readers to [14], [15] for more details. Note that the subscript  $i$  is omitted in variables for simplicity.

The attitude error is:

$$[q_{e,w}, q_{e,x}, q_{e,y}, q_{e,z}]^T = \mathbf{q}_{ref} \otimes \mathbf{q}^{-1}, \quad (25)$$

$$\tilde{\mathbf{q}}_{e,xy} = \frac{1}{\sqrt{q_{e,w}^2 + q_{e,z}^2}} \begin{bmatrix} q_{e,w}q_{e,x} - q_{e,y}q_{e,z} \\ q_{e,w}q_{e,y} + q_{e,x}q_{e,z} \\ 0 \end{bmatrix}, \quad (26)$$

$$\tilde{\mathbf{q}}_{e,z} = \frac{1}{\sqrt{q_{e,w}^2 + q_{e,z}^2}} [0 \ 0 \ q_{e,z}]^T. \quad (27)$$

The following tilt-prioritized attitude law is applied to calculate the angular acceleration command of each UAV:

$$\begin{aligned} \dot{\boldsymbol{\omega}}_d^B &= k_{q,xy} \tilde{\mathbf{q}}_{e,xy} + k_{q,z} \text{sgn}(q_{e,w}) \tilde{\mathbf{q}}_{e,z} \\ &\quad + K_{rate} (\boldsymbol{\omega}_{ref}^B - \boldsymbol{\omega}^B) \end{aligned} \quad (28)$$

By substituting  $\dot{\boldsymbol{\omega}}_d^B$  for  $\dot{\boldsymbol{\omega}}_i^{B_i}$  in (10), we can obtain the desired torque command  $\boldsymbol{\tau}_d$ . As for collective thrust, we set desired force

$$f_d = f_{ref} \quad (29)$$

Given the control-effective matrix of each UAV, knowing  $\boldsymbol{\tau}_d$  and  $f_d$  can further generate actuator commands. Details are omitted here.

## IV. VALIDATION

### A. Implementation details

- Programming environment: ROS2, Python
- NMPC solver: ACADOS, HPIPM, real-time RTK.

### B. Simulation results

Without generality, we demonstrate a case where four UAVs are manipulating a rigid-body load. The load mass is 4kg, and each UAV weighs 1kg. The cables connecting each UAV and the load are 4m. The simulation results are presented in Fig. 2 - Fig. 5.

## V. CONCLUSION

This draft introduces a centralized nonlinear model predictive control method for full-pose manipulation of a cable-suspended load using multiple UAVs. We have validated the control algorithm through numerical validations. Future works will include analysis of parameter uncertainties and real-world experimental validations.

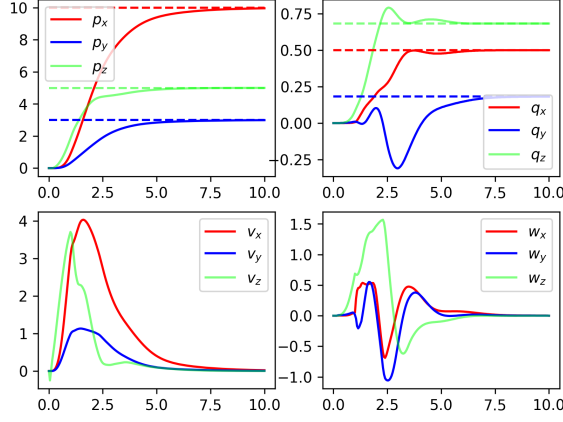


Fig. 2. Time history of the position, orientation, velocity, and angular rate of the load being manipulated by 4 UAVs. The target load position  $\mathbf{p} = [10.0, 3.0, 5.0]\text{m}$  and the target load orientation is  $[\text{roll}, \text{pitch}, \text{yaw}] = [30, 60, 90]\text{deg}$  (euler angles). Dash lines in these figures represent the reference.

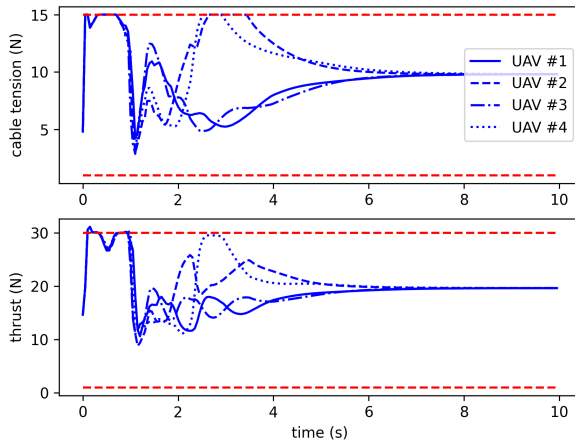


Fig. 3. Time history of the cable tension and the collective thrust of all UAVs. Red-dash lines represent the constraints. All cable and thrust-related constraints are satisfied.

## REFERENCES

- [1] S. Dai, T. Lee, and D. S. Bernstein, “Adaptive control of a quadrotor uav transporting a cable-suspended load with unknown mass,” in *53rd IEEE Conference on Decision and Control*, pp. 6149–6154, IEEE, 2014.
- [2] P. Foehn, D. Falanga, N. Kuppuswamy, R. Tedrake, and D. Scaramuzza, “Fast trajectory optimization for agile quadrotor maneuvers with a cable-suspended payload,” 2017.
- [3] G. Tartaglione, E. D’Amato, M. Ariola, P. S. Rossi, and T. A. Johansen, “Model predictive control for a multi-body slung-load system,” *Robotics and Autonomous Systems*, vol. 92, pp. 1–11, 2017.
- [4] I. Moreno Caireta, “Planning and control of a multiple-quadcopter system cooperatively carrying a slung payload in dynamical environments. a centralized model predictive control solution,” B.S. thesis, Universitat Politècnica de Catalunya, 2018.
- [5] M. Romano, A. Ye, J. Pye, and E. Atkins, “Cooperative multilift slung load transportation using haptic admittance control guidance,” *Journal of Guidance, Control, and Dynamics*, vol. 45, no. 10, pp. 1899–1912, 2022.

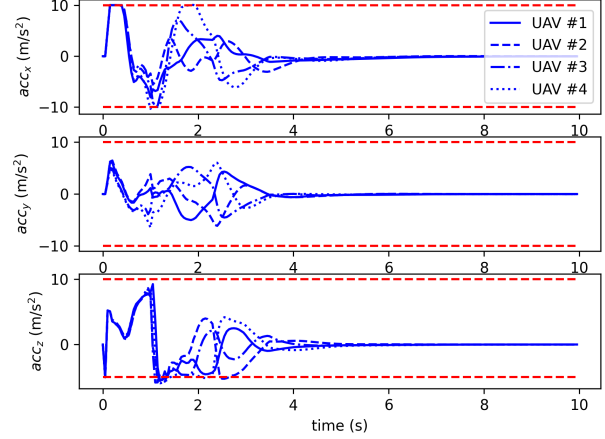


Fig. 4. Time history of the acceleration of all UAVs. Red-dash lines represent the constraints. All acceleration constraints are satisfied.

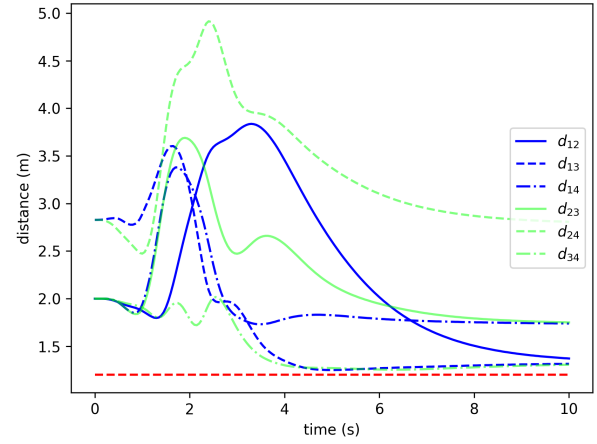


Fig. 5. Time history of the relative distances between UAVs. Red-dash lines represent the minimum distance (1.2m) set in the controller.

- [6] T. Lee, “Geometric control of quadrotor uavs transporting a cable-suspended rigid body,” *IEEE Transactions on Control Systems Technology*, vol. 26, no. 1, pp. 255–264, 2017.
- [7] G. Li, X. Liu, and G. Loianno, “Rotortm: A flexible simulator for aerial transportation and manipulation,” *arXiv preprint arXiv:2205.05140*, 2022.
- [8] D. Sanalitro, H. J. Savino, M. Tognon, J. Cortés, and A. Franchi, “Full-pose manipulation control of a cable-suspended load with multiple uavs under uncertainties,” *IEEE Robotics and Automation Letters*, vol. 5, no. 2, pp. 2185–2191, 2020.
- [9] N. Michael, J. Fink, and V. Kumar, “Cooperative manipulation and transportation with aerial robots,” *Autonomous Robots*, vol. 30, no. 1, pp. 73–86, 2011.
- [10] K. Sreenath, N. Michael, and V. Kumar, “Trajectory generation and control of a quadrotor with a cable-suspended load-a differentially-flat hybrid system,” in *2013 IEEE international conference on robotics and automation*, pp. 4888–4895, IEEE, 2013.
- [11] D. Falanga, P. Foehn, P. Lu, and D. Scaramuzza, “Pampc: Perception-aware model predictive control for quadrotors,” in *2018 IEEE/RSJ International Conference on Intelligent Robots and Systems (IROS)*, pp. 1–8, IEEE, 2018.
- [12] T. Lee, M. Leok, and N. H. McClamroch, “Geometric tracking control of a quadrotor uav on se (3),” in *49th IEEE conference on decision*

*and control (CDC)*, pp. 5420–5425, IEEE, 2010.

- [13] E. Fresk and G. Nikolakopoulos, “Full quaternion based attitude control for a quadrotor,” in *2013 European control conference (ECC)*, pp. 3864–3869, IEEE, 2013.
- [14] D. Brescianini and R. D’Andrea, “Tilt-prioritized quadrocopter attitude control,” *IEEE Transactions on Control Systems Technology*, vol. 28, no. 2, pp. 376–387, 2018.
- [15] S. Sun, A. Romero, P. Foehn, E. Kaufmann, and D. Scaramuzza, “A comparative study of nonlinear mpc and differential-flatness-based control for quadrotor agile flight,” *IEEE Transactions on Robotics*, vol. 38, no. 6, pp. 3357–3373, 2022.